RSC Advances

PAPER

View Article Online
View Journal | View Issue

Cite this: *RSC Adv.*, 2020, **10**, 34712

Co^0 superparamagnetic nanoparticles stabilized by an organic layer coating with antimicrobial activity

Paula A. Santana,[a] Carolina A. Castillo, *[a] Sebastián A. Michea,[a] Diego Venegas-Yazigi [bc] and Verónica Paredes-García [bd]

Cobalt (Co) is one of the most promising materials in nanotechnology due to its superior magnetic properties. However, due to the high cytotoxicity of cobalt, the activity in biological systems has been little studied. In this work, we report the structural, morphological, and magnetic properties of cobalt nanoparticles stabilized with an organic layer (Co^0@C-NPs) and its potential antimicrobial activity. The Co^0@C-NPs were obtained from solvothermal conditions and characterized by X-ray powder diffraction, electronic microscopy, and magnetic measurements. The organic layer was analysed by thermogravimetric analysis, Scanning Electron Microscopy, Energy Dispersive Spectrometer, and Fourier Transform Infrared Spectroscopy. From the TEM image, an organic coating layer is observed around Co^0 where this coating prevents NPs from oxidation allowing it to remain stable until 400 °C. Surface composition studies by SEM/EDS allowed the identification of carbon, oxygen, and cobalt elements present in the organic layer. This result was corroborated later by FITR analysis. Preliminary antibacterial properties were also investigated, which showed that the cobalt nanoparticles are active against *Staphylococcus aureus* after 1 h of exposure. The superparamagnetic properties and organic coating Co^0@C-NPs could be biocompatible with biological systems, but more research is needed to apply these nanoparticles in biomedical products.

Received 14th August 2020
Accepted 11th September 2020

DOI: 10.1039/d0ra07017c

rsc.li/rsc-advances

Introduction

Magnetic nanoparticles (MNPs) have attracted attention due to their potential applications in a wide range of technologies, including environmental remediation, catalysis, magnetic fluids, and magnetic resonance imaging.[1–3] In the field of nanotechnology and nanomedicine, magnetic nanoparticles are of interest to researchers in studies of hyperthermia therapy, temperature-triggered drug release,[4,5] and cytotoxicity on cancer cells,[6] because of their unique physical and chemical properties.[7,8] Small sizes and large surface area to volume ratios make nanomaterials very reactive and enable them to interact with the cell wall and genome of bacteria, leading to their antimicrobial activity.[9] Among the MNPs, cobalt (Co) is one of the most promising materials and has attracted a great deal of interest for many years from researchers from a wide range of fields for different applications.[10] Co nanoparticles exhibit high resistance to oxidation, corrosion, and wear.[11] Most importantly, Co-NPs also have an intrinsic advantage in biomedical related fields.[10] Due to their superior magnetic properties, Co nanoparticles could be a promising candidate for biomedical applications substituting the almost uniquely used biocompatible iron oxide nanoparticles.[5] The activity in biological systems of Co-NPs and nanocomposites has been little studied. Because Co has high cytotoxicity, its passivation with an inert shell is a necessary prerequisite.[6] However, some publications show that cobalt nanoparticles and cobalt oxide nanoparticles have been used as antitumor, anticancer, and antimicrobial agents.[7,10–12] Also, they have been tested as nanotherapeutic agents against the proliferation of *Acanthamoeba castellani*,[13] an amoeba that can be found in most ecosystems and is responsible for causing many diseases in humans.[14] Other studies have published positive results of the antimicrobial action of cobalt cellulose nanocomposite against Gram-positive and Gram-negative bacteria.[15] *Staphylococcus aureus* is a pathogen responsible for serious infections, which can often be treated with broad-spectrum antibiotics. However, due to the growing concern of antimicrobial resistance, alternative antimicrobials are needed.[15] Besides, little information is available in the literature on the antimicrobial activity of metallic cobalt nanoparticles (Co^0-NPs). However, studies show the use of complex nanostructured systems based on cobalt, such as, for example; rare earth element (REE) cerium (Ce^{3+}) doped $CoFe_2O_4$ nanoparticles,[16] nitrogen-rich carbon-coated bismuth/cobalt

[a]*Universidad Autónoma de Chile, Instituto de Ciencias Químicas Aplicadas, Facultad de Ingeniería, El Llano Subercaseaux 2801, San Miguel, Santiago 8910060, Chile. E-mail: carolina.castillo@uautonoma.cl*

[b]*CEDENNA, Santiago, Chile*

[c]*Universidad de Santiago de Chile, Facultad de Química y Biología, Departamento de Química de los Materiales, Santiago, Chile*

[d]*Universidad Andrés Bello, Facultad de Ciencias Exactas, Departamento de Ciencias Químicas, Santiago, Chile*

nanoparticles,[17] cobalt ferrite-chitosan,[18] and Co-doped TiO_2 nanostructures,[19] which have presented good antimicrobial behavior in Gram-positive and Gram-negative bacteria. Many synthetic methods have been developed to prepare MNPs, including the thermal decomposition method,[20] hydrothermal microemulsion process,[21] high temperature solution phase method,[22] and solvothermal process.[23] Solvothermal synthesis has allowed obtaining stable cobalt nanoparticles (Co^0-NPs) with sizes smaller than 20 nm and spherical shape.[24] Thus, the aim of this study was to develop stable and superparamagnetic Co^0@C-NPs through solvothermal technique and analyzed its antimicrobial activity against *Staphylococcus aureus*.

Experimental

Materials

All the starting materials were commercially available reagents of analytical grade and were used without further purification.

Synthesis of Co^0@C-NPs

The Co^0@C-NPs were obtained using solvothermal synthesis in the same synthetic conditions, as reported by Paredes-Garcia *et al.*[23] Due to the high stability obtained in nickel nanoparticles synthesis. The NPs were obtained from L-2-amino-3-hydroxypropanoic acid (L-serine) and $CoCl_2 \cdot 6H_2O$ in a molar ratio of 1 : 1, using DMF in a 23 mL Teflon-lined stainless steel autoclave.

Characterization

The Co^0@C-NPs were characterized by powder X-ray diffraction (PXRD) using a Bruker diffractometer, model D8 Advance with Cu Kα1 radiation and Bragg–Brentano geometry in the $5 \leq 2q \leq 80$ range. The morphological features of nanoparticles were observed by Transmission Electron Microscope (TEM) model JEM-1001L and Scanning Electron Microscope (SEM) Zeiss EVO MA10 equiped with an Oxford X-Act Energy Dispersive Spectrometer (EDS). A Vibrating Sample Magnetometer (VSM) PPMS Dyna Cool 9T was used to characterize the magnetic properties of as-prepared nanoparticles. The nanoparticles stability was study through Thermogravimetric Analysis (TGA) on PerkinElmer Thermogravimetric Analyzer, model TGA4000. The FTIR spectroscopy technique was used for identify and characterize the organic coating on Fourier Transform Infrared Spectrometer Jasco FT/IR-4600.

Antibacterial activity

Staphylococcus aureus (ATCC 25923) was provided by the Chilean Institute of Public Health (ISP). The strain was cultured overnight in trypticase soy broth (TSB) at 37 °C. Afterwards, the culture was diluted 100-fold with TSB and incubated at 200 rpm until obtaining an optical density (OD) 600 nm of mid-log phase. Cells were then washed and recovered by centrifugation at 1000 × *g* for 2 min. The resultant pellet was resuspended in 1% TSB in 10 mM phosphate buffer saline (PBS) and adjusted to 1×10^7 CFU mL^{-1} (between 0.1 to 0.7 corresponding to 1×10^7 CFU mL^{-1}). Then was exposed to 0.5, 1, and 2 mM Co^0@C-NPs concentrations for 1 h at optimum growth temperature. Following exposure, the bacteria culture was diluted ten-fold with the same buffer and incubated for 18 h in fresh TSB media. Independent experiments were repeated a minimum of three times.[25]

Scanning Electron Microscopy (SEM) of Gram positive bacteria

Aliquots 100 μL of mid-log phase *S. aureus* was harvested by centrifugation at 3000 × *g* for 5 min and resuspended in HEPES buffer 10 mM with 1%TSB. The cell suspension was incubated at 37 °C for 30 minutes with the Co^0@C-NPs at 0.5 and 2 mM. After incubation, the cells were centrifuged and washed 3 times at 4000 × *g* for 5 min with PBS and resuspended in the same buffer. The bacterial pellet was deposited on a glass coverslip and Gram stained. Afterwards it was sputter coated with approximately 30 nm thickness of gold. Finally, the microscopic examination was performed in a Carl Zeiss EVO MA 10 scanning electron microscope at 20 kV.

Statistical analysis

All values obtain throught antimicrobial assay were expressed as mean ± S.E. Statistical differences between means were calculated with GraphPad Prism 6 software by using the Student's *t* test correcting for differences in sample variance.

Results and discussion

Characterization of Co^0@C-NPs

X-ray powder diffraction. The chemical nature and crystallinity of the synthesized product were identified by X-ray powder diffraction. Fig. 1 show the diffraction patterns obtained for the Co^0@C-NPs. The nanoparticles display three peaks of different intensity at 2*q* values of 44.2; 51.5 and 75.8° which correspond to the Miller Indices (111), (200), (220) respectively, and are characteristic of face centered cubic Co^0 (JCPDS file no. 15-0806, cubic system, spatial group: *Fm*3*m*, $a = 3.5447$ Å). Only one metallic phase is observed.

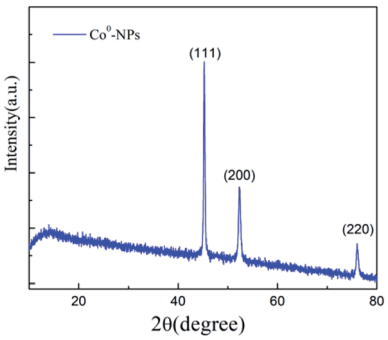

Fig. 1 Powder diffraction pattern of Co^0@C-NPs.

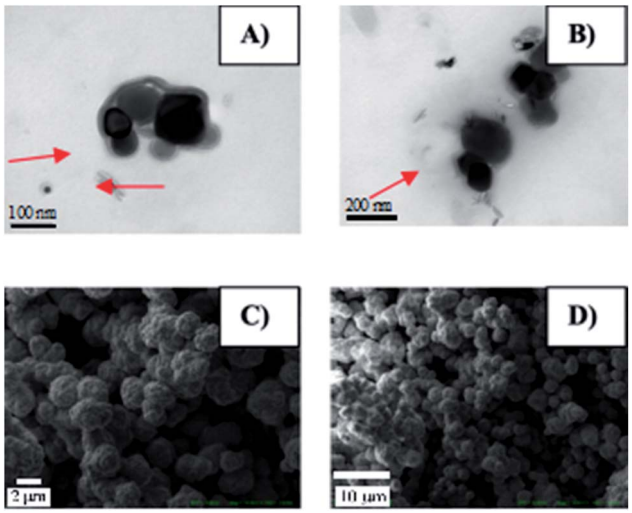

Fig. 2 Morphology of Co^0@C-NPs. (A) and (B) TEM images of Co@C^0-NPs. The organic layer is show in red arrows. (C) and (D) shows the SEM images for Co@C^0-NPs at two different magnifications.

TEM and SEM microscopy analysis of Co^0@C-NPs

Morphological and structural details of Co^0@C-NPs were investigated by scanning and transmission electron microscopy. The observation of TEM images of these nanoparticles revealed that all the particles have spherical shape with an average diameter less than 100 nm. Besides, the TEM micrographic (Fig. 2A and B) permits the observation of a thin organic coating layer. This layer was supposedly associated with the amino acid used as a starting material in a previous study, which was also responsible for the stability of the nickel nanoparticles and prevented their oxidation.[23,24] Fig. 2C and D show the SEM images for Co^0@C-NPs at two different magnifications. It is observed that they are forming homogeneous metallic agglomerates with spherical shapes and sizes around 2 μm in diameter.

In order to investigate the surface composition of the organic layer attached to the synthesized Co^0@C-NPs organic layer SEM/EDS and FTIR analysis were carried out. Through spectra obtained by SEM/EDS we observed peaks corresponding to carbon, oxygen and cobalt elements (Fig. 3).

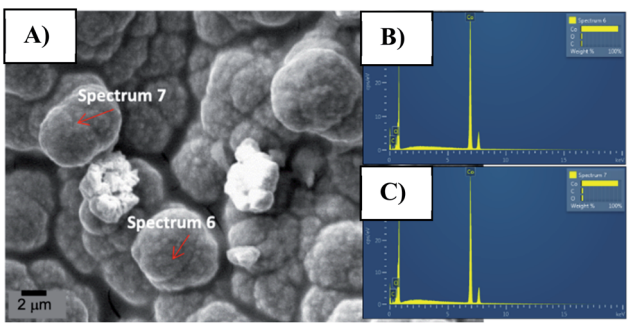

Fig. 3 Characterization of Co^0@C-NPs organic layer. SEM/EDS for Co^0@C-NPs is shown in (A). This image was used to Co^0@C-NPs surface composition studies where was obtained two spectra: 6 (B) and 7 (C). Both showed intensity peak for carbon, oxygen and cobalt elements.

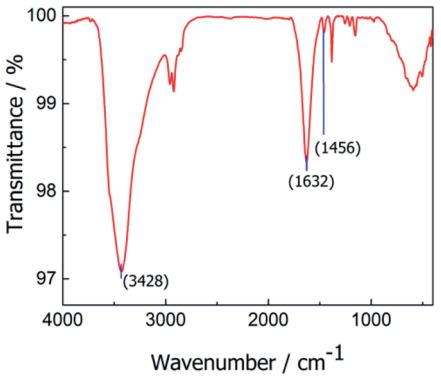

Fig. 4 Characterization of Co^0@C-NPs organic layer. FTIR spectra of Co^0@C-NPs.

The presence of organic material on the Co^0@C-NPs surface was confirmed by FTIR spectrum (Fig. 4), where we can see characteristic bands for the functional groups of amino acid. The peak noticed at 3428 cm^{-1} could be attributed to (–NH stretching)[26] 1632 cm^{-1} and 1456 cm^{-1} vibration band could be are ascribed to COO- asymmetric (u_{as}) and COO– symmetric (u_s) stretching respectively.[27–29]

Thermogravimetric analysis

In order to investigate the thermal stability, Co^0@C-NPs were subjected to thermogravimetric analysis (TGA) from 30 to 800 °C under air and nitrogen condition at the heating rate of 10 °C min^{-1}. TGA curves show that Co^0@C-NPs are stable until 400 °C (Fig. 5). Over this temperature was observed a significant mass increase of 30.32% and 26.00% in air and nitrogen atmosphere, respectively. This mass increase could be attributed to the generation of cobalt oxides due to the decomposition of organic material present in the Co^0@C-NPs surface, which is corroborated with the results obtained through TEM, SEM/EDS images and FTIR spectrum.

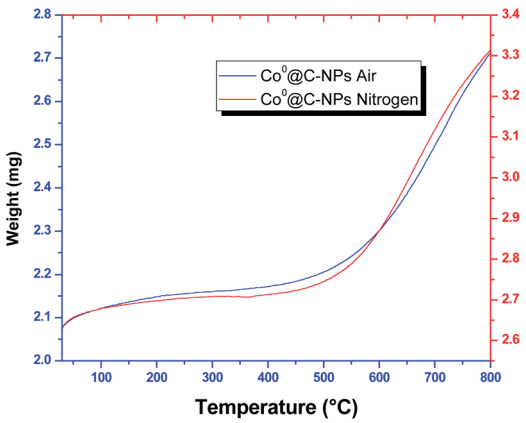

Fig. 5 TGA curve of Co^0@C-NPs.

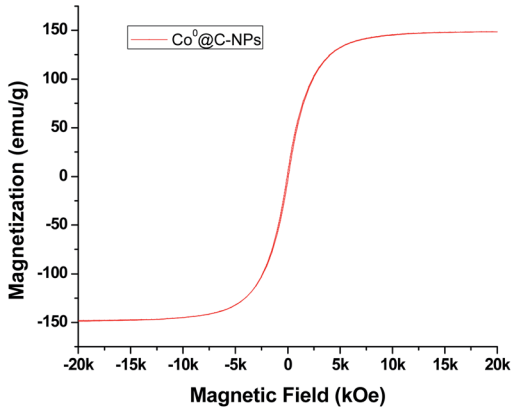

Fig. 6 Magnetization curve of Co^0@C-NPs measured at 300 K.

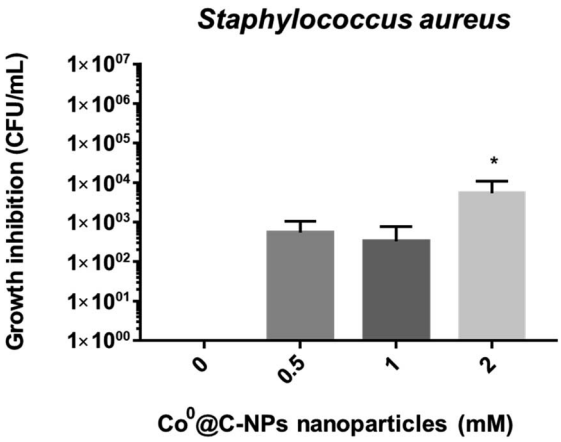

Fig. 7 Antimicrobial activity of Co^0@C-NPs. Growth inhibition of *S. aureus* in the absence of Co^0@C-NPs and in the presence of Co^0@C-NPs concentrations of 0.5, 1 and 2 mM after 1 hour of exposure. The standard error was determined from the results of two experiments carried out in triplicate.

Magnetic characterization

The magnetic behaviour for Co^0@C-NPs was investigated by vibrating sample magnetometer at 300 K under an external magnetic field sweeping from +20 to −20 kOe. The magnetic hysteresis loop for Co^0 nanoparticles is shown in Fig. 6.

The magnetic parameters values obtained from Co^0@C-NPs such as saturation magnetization (M_s), coercivity (H_c), remnant magnetization (M_r) and ratio of the remnant to saturation magnetization (M_r/M_s) are 148.6 (emu g^{-1}), 56 (Oe), 3.95 (emu g^{-1}) and 0.027 respectively. The results demonstrate that the magnetization curve shows typical superparamagnetic behavior with very low values in both remnant magnetization and coercivity. The value of M_s for Co^0@C-NPs is lower than multidomain bulk particles of Co (168 emu g^{-1}).[30] This is due to the size in which the nanoparticles are obtained. The coercive force (H_c = 56 Oe) and residual magnetization (M_r = 3.95 emu g^{-1}) are small, which indicates the Co^0@C-NPs are close to superparamagnetic. Furthermore, the ratio of M_r/M_s = 0.027, is very small, which is typical for superparamagnetic behaviour.[31] Superparamagnetic nanoparticles exhibit a monodomain structure with a high magnetic susceptibility exclusively under an external magnetic field. This unique property combining with a biocompatible capability is very promising because allow applying this kind of nanostructure in several biomedical application like theragnostic, hyperthermia tumor therapy, drug delivery, and magnetic resonance imaging.[32–34]

Antimicrobial effect of Co^0@C-NPs in bacteria

Since it has been shown that bacteria are becoming resistant to antimicrobial agents, it is necessary to find novel materials with antimicrobial activity. Nanoparticles are being used with this purpose.[35,36] The Co based nanoparticles has been studies against *Staphylococcus aureus,* these include cobalt ferrite nanoparticles[37–40] and cobalt oxide nanoparticles,[41,42] but there are a few investigation that used only metallic cobalt nanoparticles without conjugated at other nanoparticles or nanomaterials. For this reason, in this study, we evaluated the antimicrobial properties of Co^0@C-NPs synthesized by a solvothermal technique against Gram-positive bacteria (*S. aureus*) (Fig. 7). At 0.5 and 1 mM of Co^0@C-NPs, no significant inhibition was observed in the growth of *S. aureus*, but at 2 mM, it was observed that Co^0@C-NPs have major antimicrobial activity against this strain (Fig. 7), inhibiting the amount of bacteria from 0 up to 5.5×10^3 CFU mL^{-1} after 1 h of exposition. In two investigations have been demostrated that Co^0-NPs have antimicrobial activity. One of them have described that cobalt nanoparticles, in the range of 20-49 nm synthetized by adopting an eco method, showed activity against *S. aureus* above 25 mg mL^{-1},[43] which is 200 to 400 times higher than what we used in this research. The second investigation, cobalt nanoparticles of 10 nm synthetized by chemical methods are capable of killing 1×10^2 CFU mL^{-1} of *Escherichia coli* after 3 h of exposition at 1.86 mM (0.11 mg mL^{-1}), which is a lower inhibition than was obtained in this investigation.[36]

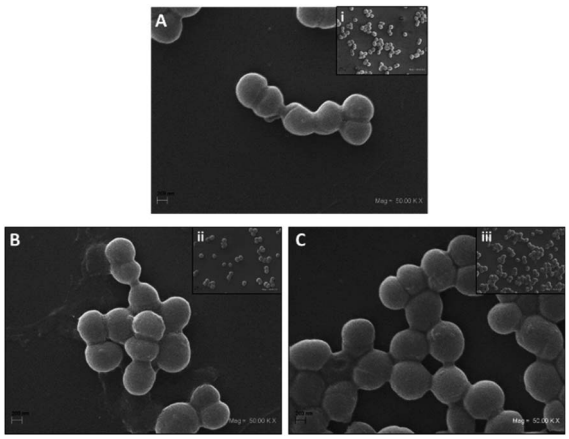

Fig. 8 Scanning electron microscopy of *S. aureus*. SEM micrographs of *Staphylococcus aureus* (A) without Co^0@C-NPs, (B) in the presence of Co^0@C-NPs at 0.5 mM, and (C) in the presence of Co^0@C-NPs at 2 mM.

A SEM study was performed for the direct observation of cell morphological changes after Co^0@C-NPs treatment at 0.5 and 2 mM. The untreated *S. aureus* cells were used as a control, exhibiting a smooth and intact surface (Fig. 8), but when we treated *S. aureus* with Co^0@C-NPs at 0.5 mM, it was observed that NPs form an aggregate-like structure on the bacteria surface. It could be presumed that this is an interaction observed between clustering of NPs and the cell surface that occurs during co-incubation and is not reflective of damage induced to the bacteria membrane as previously described by Sousa *et al.*[44] At 2 mM a similar aggregate structure was observed but with fewer NPs. Probably, since there is a higher concentration of Co^0@C-NPs, it is easier for them to aggregate and precipitate at the time of centrifugation, leaving individual NPs or apparently loose NPs aggregates[44] on the bacteria surface. Further research is necessary to demonstrate if Co^0@C-NPs have effects on bacterial surfaces or on intracellular components of bacteria at different times.

Given that Co^0@C-NPs have a thin organic coating layer associated to L-serine amino acid and DMF which is responsible for their stability and prevention of oxidation, the effect of metallic cobalt in bacterial growth-inhibition may be explained for the generation of oxidation products derived from L-serine amino acid in agreement to general reaction of oxidation for α-amino acids: $R{\cdot}CH(NH_2){\cdot}CO_2H + O \rightarrow R{\cdot}CHO + NH_3 + CO_2$ described by Hough *et al.*[45,46] and oxidation of DMF to a carboxylic acid as well as the reduction of Ni^{2+} (or Co^{2+}) to Ni (or Co), which can be briefly formulated as follows: $HCONMe_2 + Ni^{2+}(\text{or } Co^{2+}) + H_2O \rightarrow Ni(\text{or Co}) + Me_2NCOOH + 2H^+$ described by Zhang *et al.*,[46] where functional groups of Me_2NCOOH could be able to form hydrogen bonds with the bacterial cell wall.

On the other hand, it has been described that different types of nanoparticles generate reactive oxygen species (ROS), that could damage bacterial DNA, cell membranes (lipid peroxidation) and cause protein dysfunction.[15,35,47,48] In this study, cobalt ions could be released from metallic cobalt nanoclusters which could interact with thiol groups on bacterial enzymes leading to cell death, as previously described by Alahmadi *et al.*[47] Further experiments are essential before concluding about the antibacterial behavior of such oxidation products generated in the synthesis of Co^0@C-NPs, which may lead to the release of cobalt ions or possibly both. Experiments will be important for determining the potential use of these nanoparticles as a new antimicrobial agent to combat bacterial infections.

Conclusions

In conclusion, we report the structural, morphological and magnetic properties of cobalt nanoparticles stabilized with an organic layer (Co^0@C-NPs) and its potential antimicrobial activity. The solvothermal technique permits us to obtain stable and spherical fcc-Co^0 with an organic layer that avoids the oxidation process until 400 °C. The elemental analysis confirm the presence of carbon and oxygen elements associated to organic layer and through spectroscopy was identified functional groups of amino acid like –NH and COO–.

Furthermore, this study reveals promissory results given that Co^0@C-NPs shows antimicrobial activity against *S. aureus* at 2 mM, being 55 times more effective in less time than the previous studies. SEM analysis shows that Co^0@C-NPs form an aggregate-like structure probably due interaction observed between clustering of NPs and the cell surface. Further research is necessary to establish the mechanism of action of the Co^0@C-NPs.

The organic coating Co^0@C-NPs and superparamagnetic property could be biocompatible with biological systems and in the future could be use in several biomedical application without additional processes required such as encapsulation, but previously must be evaluated its biosafety through *in vitro* biological assay.

Conflicts of interest

The authors declare that they have no competing interest.

Acknowledgements

This work was funded by project DIUA 151-2019 from the Dirección de Investigación of Universidad Autónoma de Chile and FONDECYT project No. 11170244 and No. 11170544. Financiamiento Basal para Centros Científicos y Tecnológicos de Excelencia AFB180001 and CONICYT-FONDEQUIP/PPMS/EQM130086-UNAB.

Notes and references

1 A. H. Lu, E. L. Salabas and F. Schüth, Magnetic nanoparticles: Synthesis, protection, functionalization, and application, *Angew. Chem. Int. Ed.*, 2007, **46**(8), 1222–1244.
2 A. Gual, C. Godard, S. Castillón, D. Curulla-Ferré and C. Claver, Colloidal Ru, Co and Fe-nanoparticles. Synthesis and application as nanocatalysts in the Fischer-Tropsch process, *Catal. Today*, 2012, **183**(1), 154–171.
3 W. Baaziz, S. Begin-Colin, B. P. Pichon, I. Florea, O. Ersen, S. Zafeiratos, *et al.*, High-Density Monodispersed Cobalt Nanoparticles Filled into Multiwalled Carbon Nanotubes, *Chem. Mater.*, 2012, **24**(9), 1549–1551.
4 C. Dey, K. Baishya, A. Ghosh, M. M. Goswami and A. Ghosh, *J. Magn. Magn. Mater.*, 2016, **427**, 168–174.
5 A. Kotoulas and C. Sarafidis, Carbon-encapsulated cobalt nanoparticles: synthesis , properties , and magnetic particle hyperthermia efficiency, *J. Nanopart. Res.*, 2017, **19**, 399.
6 Z. Abdullaeva, E. Omurzak, C. Iwamoto and T. Mashimo, Onion-like carbon-encapsulated Co , Ni , and Fe magnetic nanoparticles with low cytotoxicity synthesized by a pulsed plasma in a liquid, *Carbon*, 2011, **50**(5), 1776–1785.
7 V. Dogra, G. Kaur, S. Jindal, R. Kumar, S. Kumar and N. Kumar, Science of the Total Environment Bactericidal effects of metallosurfactants based cobalt oxide/hydroxide nanoparticles against Staphylococcus aureus, *Sci. Total Environ.*, 2019, **681**, 350–364.

8 J. Z. Hilt, Magnetic nanoparticles in biomedicine: synthesis , functionalization and applications Review, *Nanomedicine*, 2010, **5**, 1401–1414.
9 D. K. Henderson, Managing Methicillin-Resistant Staphylococci: A Paradigm for Preventing Nosocomial Transmission of Resistant Organisms, *Am. J. Med*, 2006, **119**, 45–52.
10 S. M. Ansari, R. D. Bhor, K. R. Pai, D. Sen, S. Mazumder, K. Ghosh, *et al.*, Cobalt Nanoparticles for Biomedical Applications: Facile Synthesis , Physiochemical Characterization , Cytotoxicity Behavior and Biocompatibility, *Appl. Surf. Sci.*, 2017, **414**, 171–187.
11 M. Alagiri, C. Muthamizhchelvan and S. B. A. Hamid, Synthesis of superparamagnetic cobalt nanoparticles through solvothermal process, *J. Mater. Sci. Mater. Electron.*, 2013, **24**(11), 4157–4160.
12 S. Khan, A. A. Ansari, A. Arif, K. Rehan, O. Al, O. Wael, *et al.*, In vitro evaluation of anticancer and antibacterial activities of cobalt oxide nanoparticles, *J. Biol. Inorg Chem.*, 2015, **20**(8), 1319–1326.
13 A. Anwar, A. Numan, R. Siddiqui, M. Khalid and N. A. Khan, Cobalt nanoparticles as novel nanotherapeutics against Acanthamoeba castellanii, *Parasites Vectors*, 2019, 1–10.
14 J. C. Castrill and L. P. Orozco, spp. como parásitos patógenos y oportunistas, *Rev. Chil. infectol.*, 2013, **30**, 147–155.
15 N. S. Alahmadi, J. W. Betts, F. Cheng, M. G. Francesconi and S. M. Kelly, Cellulose magnetic nanocomposites, *RSC Adv.*, 2017, **7**, 20020–20026.
16 K. Elayakumar, A. Dinesh, A. Manikandan, M. Palanivelu, G. Kavitha, S. Prakash, R. Thilak Kumar, S. Jaganathan and A. Baykal, Structural, morphological, enhanced magnetic properties and antibacterial bio-medical activity of rare earth element (REE) Cerium (Ce^{3+}) doped $CoFe_2O_4$ nanoparticles, *J. Magn. Magn. Mater.*, 2018, **476**, 157–165.
17 R. Wang, B. Zhang, Z. Liang, Y. He, Z. Wang, X. Ma, *et al.*, Environmental Insights into rapid photodynamic inactivation mechanism of Staphylococcus aureus via rational design of multifunctional nitrogen-rich carbon-coated bismuth/cobalt nanoparticles, *Appl. Catal., B*, 2019, **241**, 167–177.
18 Z. E. Eldine, W. M. A. Rouby and El. PT CR., *Mater. Sci. Eng. C*, 2018, **91**, 361–371.
19 M. Hosseini-zori, Journal of Photochemistry & Photobiology , B: Biology Co-doped TiO_2 nanostructures as a strong antibacterial agent and self- cleaning cover: Synthesis , characterization and investigation of photocatalytic activity under UV irradiation, *J. Photochem. Photobiol. B Biol.*, 2018, **178**, 512–520.
20 I. C. Communication and A. D. Khalaji, Cobalt oxide nanoparticles by solid-state decomposition: Synthesis and characterization, *Chem. Commun.*, 2019, **7**, 113–116.
21 J. Yang, C. Lin, Z. Wang and J. Lin, In(OH)3 and In_2O_3 nanorod bundles and spheres: Microemulsion-mediated hydrothermal synthesis and luminescence properties, *Inorg. Chem.*, 2006, **45**(22), 8973–8979.
22 Y. Su, X. OuYang and J. Tang, Spectra study and size control of cobalt nanoparticles passivated with oleic acid and triphenylphosphine, *Appl. Surf. Sci.*, 2010, **256**(8), 2353–2356.
23 V. Paredes-Garcia, C. Cruz, N. Toledo, J. Denardin, D. Venegas-Yazigi, C. Castillo, E. Spodine and Z. Luo, Effect of the different synthetic parameters on the morphology and magnetic properties of nickel nanoparticles, *New J. Chem.*, 2014, **38**(2), 837–844.
24 C. Castillo, K. Seguin, P. Aguirre, A. D. C. Viegas and E. Spodine, Nickel nanocomposites: magnetic and catalytic, *RSC Adv.*, 2015, **5**, 63073–63079.
25 M. Azkargorta, J. Soria, C. Ojeda, F. Guzman, A. Acera, I. Iloro, T. Suárez and F. Elortza, Human basal tear peptidome characterization by CID , HCD and ETD followed by in silico and in vitro analyses for antimicrobial peptide identification, *J. Proteome Res.*, 2015, **14**(6), 2649–2658.
26 A. B. Tamboli and N. N. Maldar, Synthesis and characterization of processable aromatic poly (ether ether ketone amide) s modified by phenoxy, *Polym Bull*, 2020, 0123456789.
27 W. Lee, C. Loo, A. V. Zavgorodniy and R. Rohanizadeh, High protein adsorptive capacity of amino acid-functionalized hydroxyapatite, *J. Biomed. Mater. Res.*, 2012, 1–11.
28 M. Nageshwari, C. R. T. Kumari, G. Vinitha, S. Muthu and M. L. Caroline, *Phys. B Condens. Matter*, 2018, **541**, 32–42.
29 K. Tõnsuaadu, M. Gruselle, F. Kriisa, A. Trikkel, P. Gredin and D. Villemin, Dependence of the interaction mechanisms between l - serine and O - phospho - l - serine with calcium hydroxyapatite and copper modified hydroxyapatite in relation with the acidity of aqueous medium, *J. Biol. Inorg Chem.*, 2018, 0123456789.
30 G. Zhu, X. Wei, C. Xia and Y. Ye, Solution route to single crystalline dendritic cobalt nanostructures coated with carbon shells, *Carbon*, 2007, **45**, 1160–1166.
31 M. Galaburda, V. Bogatyrov, O. Oranska and V. Gun, Synthesis and characterization of carbon composites containing Fe , Co , Ni nanoparticles, *J. Therm. Anal. Calorim.*, 2015, **122**, 553–561.
32 S. Talluri and R. R. Malla, Superparamagnetic Iron Oxide Nanoparticles (SPIONs) for Diagnosis and Treatment of Breast , Ovarian and Cervical Cancers, *Curr. Drug Metab.*, 2019, **20**, 12.
33 E. J. Guggenheim, J. Z. Rappoport and I. Lynch, Mechanisms for cellular uptake of nanosized clinical MRI contrast agents, *Nanotoxicology*, 2020, 1–29.
34 Y. Xiao, Superparamagnetic nanoparticles for biomedical applications, *J. Mater. Chem.*, 2019, **8**, 354–367.
35 Y. N. Slavin, J. Asnis, U. O. Häfeli and H. Bach, Metal nanoparticles: understanding the mechanisms behind antibacterial activity, *J. Nanobiotechnol.*, 2017, 1–20.
36 S. Hatamie, M. Nouri, S. K. Karandikar, A. Kulkarni, S. D. Dhole, D. M. Phase and S. Kale, Complexes of cobalt nanoparticles and polyfunctional curcumin as antimicrobial agents, *Mater. Sci. Eng. C*, 2012, **32**(2), 92–97.
37 N. Sanpo, C. C. Berndt, C. Wen and J. Wang, Transition metal-substituted cobalt ferrite nanoparticles for

biomedical applications, *Acta Biomater.*, 2013, **9**(3), 5830–5837.

38 R. Žalnėravičius, A. Paškevičius, K. Mažeika and A. Jagminas, *Appl. Surf. Sci.*, 2017, **435**, 141–148.

39 V. S. Kirankumar, Photocatalytic and antibacterial activity of bismuth and copper co- doped cobalt ferrite nanoparticles, *J. Mater. Sci. Mater. Electron.*, 2018, **29**, 8738–8746.

40 S. Rehman, M. A. Ansari, M. A. Alzohairy, M. N. Alomary, B. R. Jermy, R. Shahzad, N. Tashkandi and Z. H. Alsalem, Synthesized Neodymium-Substituted Cobalt, *Processes*, 2019, **7**, 714.

41 A. Talha, M. Ovais, I. Ullah, M. Ali, Z. K. Shinwari and M. Maaza, Physical properties , biological applications and biocompatibility studies on biosynthesized single phase cobalt oxide (Co_3O_4) nanoparticles via Sageretia thea (Osbeck .), *Arabian J. Chem.*, 2020, **13**(1), 606–619.

42 V. Dogra, G. Kaur, S. Jindal, R. Kumar, S. Kumar, N. Kumar and N. K. Singhal, Bactericidal effects of metallosurfactants based cobalt oxide/hydroxide nanoparticles against Staphylococcus aureus, *Sci. Total Environ.*, 2019, **681**, 350–364.

43 O. Igwe and E. S. Ekebo, Biofabrication of cobalt nanoparticles using leaf extract of Chromonaela odorata and their potential antibacterial application, *Res. J. Chem. Sci.*, 2018, **8**, 1 11–17.

44 C. Sousa, D. Sequeira, Y. V. Kolen, I. M. Pinto and D. Y. Petrovykh, Analytical Protocols for Separation and Electron Microscopy of Nanoparticles Interacting with Bacterial Cells Analytical Protocols for Separation and Electron Microscopy of Nanoparticles Interacting with Bacterial Cells, *Anal. Chem.*, 2015, **87**, 4641–4648.

45 L. Hough and V. Slyke, The Periodate Oxidation of Amino Acids with Reference to Studies on Glycoproteins, *Biochem*, 1965, 17–24.

46 Z. Zhang, X. Chen, X. Zhang and C. Shi, Synthesis and magnetic properties of nickel and cobalt nanoparticles obtained in DMF solution, *Solid State Commun.*, 2006, **139**, 403–405.

47 A. A. Dayem, M. K. Hossain, S. B. Lee, K. Kim, S. K. Saha, G. Yang, H. Choi and S. Cho, The Role of Reactive Oxygen Species (ROS) in the Biological Activities of Metallic Nanoparticles, *Int. J. Mol. Sci.*, 2017, **18**, 120.

48 L. Wang and C. Hu, The antimicrobial activity of nanoparticles: present situation and prospects for the future, *Int. J. Nanomed.*, 2017, 1227–1249.

